

# Changes and distribution of lamellae in the spherulites of poly(ether ether ketone) upon stepwise crystallization

Tong Y. Ko and E. M. Woo\*

Department of Chemical Engineering, National Cheng Kung University, Tainan, Taiwan 701-01, ROC

(Received 15 March 1995; revised 30 June 1995)

Coexistence of multiple lamellar thicknesses and lamellar thickness changes in poly(ether ether ketone) (PEEK) have been supported by the results obtained from investigations using differential scanning calorimetry (d.s.c.), X-ray and scanning electron microscopy. The melting behaviour, crystallization kinetics and morphology of PEEK subjected to multiple-step crystallization have been studied. During stepwise crystallization of the polymer, a major lamella crystal develops first, which possesses a melting peak temperature close to the equilibrium melting temperature; however, a small fraction of the polymer is packed into minor crystal aggregates of smaller lamellar thicknesses which, upon d.s.c, display the observed phenomenon of multiple minor melting peaks located further below the main melting peak. It is this multiple distribution of lamellar thicknesses that causes multiple melting behaviour. A descriptive crystallization kinetic model is used to help explain this phenomenon by correlating the crystallization and thermal behaviour in PEEK.

(Keywords: multiple melting peaks; PEEK; crystallization kinetics)

Poly(ether ether ketone) (PEEK) is one of the most studied semicrystalline thermoplastics due to its excellent mechanical properties as a high-performance polymer for various applications and as a matrix for advanced fibre-reinforced composites<sup>1-7</sup>. Double melting endotherms in semicrystalline polymers have been observed during thermal analysis for many years, most notably in poly(ethylene terephthalate)<sup>8-11</sup>. The interpretations vary from different crystal structure or lamellar thickness, to simultaneous melting and recrystallization. Wunderlich<sup>12</sup> has provided some interesting interpretations for the possible mechanism of double melting behaviour by theorizing on melting of the minor crystal and recrystallization and remelting during scanning, while Roberts<sup>13</sup> has explained this behaviour in terms of the melting of crystals of two different sizes.

There have been many extensive studies on the multiple melting behaviour of PEEK<sup>14-17</sup>, poly(butylene terephthalate) (PBT)<sup>18,19</sup>, poly(1,4-phenylene sulfide) (PPS)<sup>20-22</sup>, and other semicrystalline polymers. Attempts to explain the origin of the multiple melting peaks in certain semicrystalline polymers have been made by various researchers. The issues remain quite controversial, however, since interpretations still vary significantly among the proposed theories. Two mechanisms have been proposed to explain the multiple melting behaviour of PEEK and other high-melting thermoplastics. Blundell<sup>14</sup> and Blundell and Osborn<sup>23</sup> proposed a

reorganization model. Later, Lee and Porter<sup>16</sup> proposed a slight modification and suggested that the melting of core crystals can be retarded by the reorganization process. However, Bassett *et al.*<sup>24</sup> suggested a dual-morphology model in which the secondary lamellae may melt at lower temperatures and the primary lamellae melt at higher temperatures. Cheng *et al.*<sup>25</sup> and Cebe and co-workers<sup>21,22</sup> have also proposed similar interpretations. In addition, Marand and Prasad<sup>26</sup> used polarized optical microscopy to study the morphology of PEEK and claimed that they found experimental evidence of two different morphologies. Typical spherulitic morphologies are present if PEEK is crystallized below 300°C, while single-crystal-aggregate structures can be observed during isothermal crystallization above 300°C. Lovinger *et al.*<sup>27</sup> have also provided experimental results to support a conclusion of dual morphologies. In one of our recent reports on PEEK, it has been proposed that the hypothesis of melting crystals during differential scanning calorimetry (d.s.c.) has been found to be less likely<sup>28</sup>.

A large number of melting peaks can be observed between the glass transition temperature ( $T_g$ ) and the highest melting temperature ( $T_m$ ) (345°C) if PEEK is subjected to prescribed stepwise isothermal treatments after being quenched from the melt state above the melting temperature. The multiple melting behaviour thus appears to be quite complex. Can we explain this phenomenon in terms of melting of crystals with an infinite number of sizes? The objective of this study was to provide thermal, crystallographic, morphological and crystallization kinetic modelling evidence to explain these interesting observations.

\* To whom correspondence should be addressed

## EXPERIMENTAL

*Materials and sample preparation*

PEEK ( $M_n = 14\,000 \text{ g mol}^{-1}$ , ICI) was obtained in a high-purity, additive-free film form. The main starting polymer specimens were PEEK films isothermally cold- or melt-crystallized at a single isothermal temperature or multiply crystallized stepwise at a series of progressively descending isothermal temperatures. The multiply crystallized specimens were then subjected to various prescribed thermal treatments, described in more detail in the Results and discussion section. All crystallization and thermal treatments of PEEK were performed in the cell of the differential scanning calorimeter, therefore the temperature accuracy and control for annealing or crystallization of the polymer samples was excellent.

*Differential scanning calorimetry*

A power-compensated type of differential scanning calorimeter (Perkin-Elmer DSC 7, equipped with an intracooler and a computer for data acquisition/analysis) was used for various thermal treatments (quenching, annealing, cold- or melt-crystallization) of the samples and to observe the melting endothermic peaks. The temperature and heat of melting were calibrated with a high-purity indium standard. Relatively small sample sizes (2–4 mg) were used to minimize the effect of low thermal conductivities of the polymers. For determination of melting points, the polymer samples were scanned from ambient temperature to approximately  $25^\circ\text{C}$  above the respective melting temperature of each polymer at a scanning rate of  $10^\circ\text{C min}^{-1}$ , unless otherwise indicated. A nitrogen purge was provided throughout the thermal treatments and d.s.c. In thermal treatments of the samples, the fastest heating rate ( $+300^\circ\text{C min}^{-1}$ ) or cooling rate ( $-320^\circ\text{C min}^{-1}$ ) was used wherever needed in excluding complicating factors from non-isothermal crystallization.

*Wide-angle X-ray diffraction (WAXD)*

The X-ray instrument used was Rigaku D/Max II-B with copper  $K\alpha$  radiation and a wavelength of  $1.542 \text{ \AA}$ . PEEK specimens were prepared with various thermal treatments or crystallization by methods similar to those described for the thermal analysis samples. X-ray diffraction was performed to examine possible differences in the crystal perfection in the lamellar structure or alteration of the crystals in the PEEK samples prepared with various thermal treatments or crystallization methods.

*Scanning electron microscopy (SEM)*

The morphology of the PEEK samples was examined using a scanning electron microscope (JEOL JSM-35). The crystallized/annealed PEEK samples were first etched with potassium permanganate solution and subsequently coated with gold by vapour deposition using a vacuum sputterer.

## RESULTS AND DISCUSSION

Figure 1 shows the d.s.c. scans at  $10^\circ\text{C min}^{-1}$  of various PEEK samples that were quenched from the melt state and subjected to isothermal crystallization (for 30 min) at 230, 250, 270, 290 and  $310^\circ\text{C}$ . In addition to the main

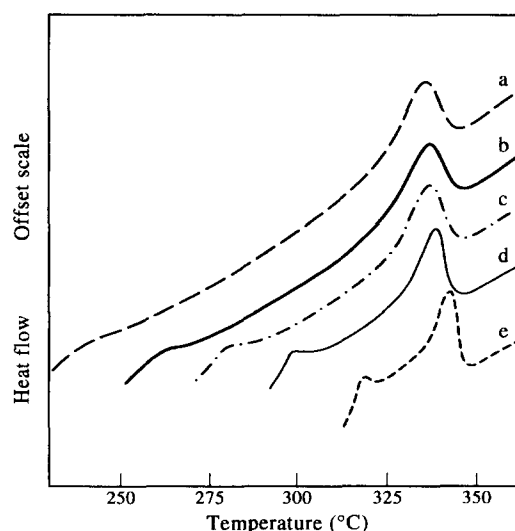
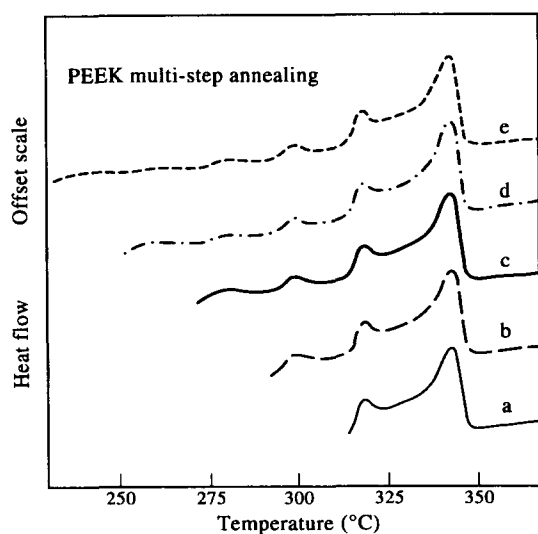


Figure 1 Melting behaviour of PEEK crystallized for 30 min at various temperatures: (a)  $230^\circ\text{C}$ ; (b)  $250^\circ\text{C}$ ; (c)  $270^\circ\text{C}$ ; (d)  $290^\circ\text{C}$ ; (e)  $310^\circ\text{C}$

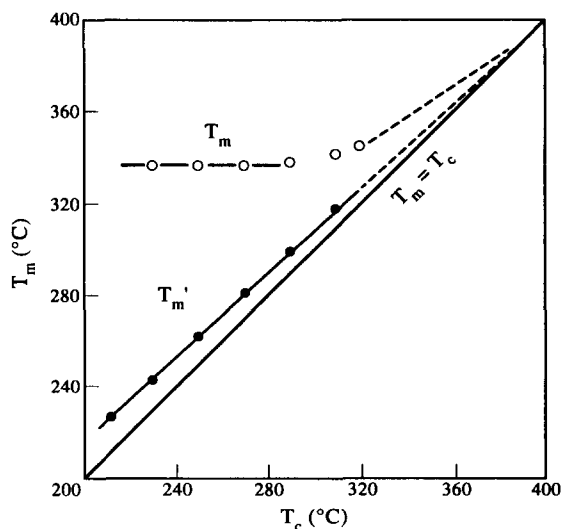
melting peak, a minor endothermic peak can be clearly identified in each thermogram slightly above the respective crystallization temperature. Interestingly, the peak temperature of the main melting endotherm appears to be independent of the isothermal crystallization temperature or time as long as the crystallization temperature is below  $300^\circ\text{C}$ . By contrast, the minor peak temperature is strongly dependent on the crystallization temperature used and the hold time at that temperature. Furthermore, the shape and intensity of this minor peak are also affected by the isothermal temperature. At the higher isothermal crystallization temperatures, the minor peak tends to be sharper, indicating that the minor crystal entities responsible for that particular minor peak exhibited a narrower distribution (sharper peak) at a higher crystallization temperature. The results clearly show that crystallization of PEEK at one temperature produces one minor peak in addition to the main melting peak upon d.s.c. Therefore, when PEEK samples were crystallized at multiple descending temperature steps, multiple minor peaks in addition to the main melting could be expected.

Figure 2 shows the d.s.c. scans at  $10^\circ\text{C min}^{-1}$  of five PEEK samples that were crystallized at 30 min at each temperature. It has been proposed in one of our recent reports<sup>28</sup> that the minor peaks are related to melting of the minor crystal lamellae, and that multiple lamellae thicknesses are more likely responsible for the multiple minor melting peaks in PEEK.

In Figure 3 both the main and minor melting peaks of the PEEK samples crystallized at various isothermal temperatures for 30 min are plotted as functions of the isothermal crystallization temperatures used. As in Figure 1, a minor peak was seen to occur above the crystallization temperature and the minor peak temperature was found to increase almost linearly with the crystallization temperature. The difference between this minor melting peak and the isothermal crystallization temperature decreased gradually with the increase in crystallization temperature. Figure 3 shows that the minor peak temperatures were extrapolated to intercept the  $T_m = T_c$  (crystallization temperature) line at



**Figure 2** D.s.c. scans showing the multiple melting behaviour of PEEK crystallized stepwise at isothermal temperatures for 30 min at each step: (a) 310°C; (b) 310 and 290°C; (c) 310, 290 and 270°C; (d) 310, 290, 270 and 250°C; (e) 310, 290, 270, 250 and 230°C



**Figure 3** Major and minor melting peaks as functions of crystallization temperature. The dashed lines show the extrapolated trends

approximately 390°C. By contrast, the peak temperature of the main melting endotherm seems to be independent of the isothermal crystallization below 300°C. At crystallization temperatures above 300°C, however, our d.s.c. results showed that the main melting peak started to increase with the crystallization temperature used. Although our data for the main melting peaks were not sufficient to show a quantitative trend, it has been reported by Lee and Porter<sup>16</sup> that, by extrapolating the main melting peak temperature to intercept the  $T_m = T_c$  line, the thermodynamic melting peak of PEEK is found to be 384°C. Clearly, the increase in the main melting peak with the crystallization temperature is related to main lamellae of greater thicknesses, which according to Lee and Porter<sup>16</sup> can thicken only at high enough crystallization temperatures. Similarly, the minor crystal lamellae also exhibited multiple thicknesses and could thicken with time when held at an isothermal crystallization

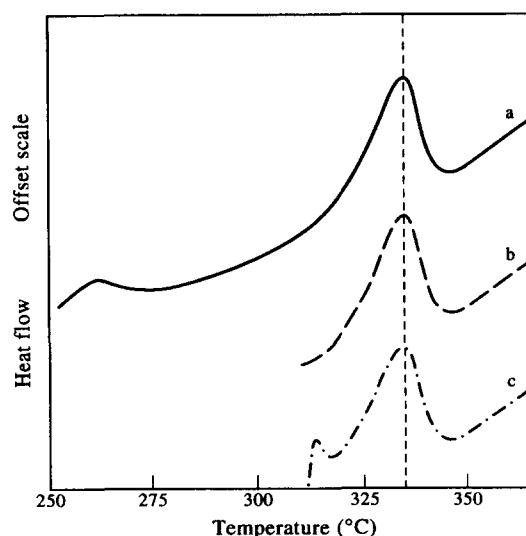


**Figure 4** Various d.s.c. scans ( $10^{\circ}\text{C min}^{-1}$ ) of PEEK crystallized at 250°C for 30 min: (a) 250–375°C at  $10^{\circ}\text{C min}^{-1}$ ; (b) 250–310°C at  $500^{\circ}\text{C min}^{-1}$ , then 310–375°C at  $10^{\circ}\text{C min}^{-1}$ ; (c) 250–310°C at  $2^{\circ}\text{C min}^{-1}$ , then 310–375°C at  $10^{\circ}\text{C min}^{-1}$

temperature for long enough times or during dynamic scanning at slow rates. This can be seen by extrapolation of the minor peak temperatures, which yielded the ultimate melting peak temperature of the minor crystal between 390 and 400°C. The fact that both the main and minor melting peak temperatures could be extrapolated to about the same value suggests that both types of lamellae can thicken ultimately to the same equilibrium dimensions under appropriate conditions.

If multiple crystal lamellae are indeed responsible for the multiple melting peaks, the melting of the minor peak(s) should be expected to be independent and the melting of the low-temperature peak(s) should not affect the area or location of the main melting peak. To show that the melting of the minor peak did not affect the main melting peak, we performed three d.s.c. scans on several PEEK samples in order to provide such evidence. *Figure 4* shows the d.s.c. scans (curves a, b and c) of the PEEK samples that had all been crystallized at 250°C for 30 min prior to the final d.s.c. heating scans. Curve a in *Figure 4* represents the PEEK sample scanned with a uniform heating rate of  $10^{\circ}\text{C min}^{-1}$  from 250 to 375°C. This thermogram reveals a main melting peak and a low-temperature minor peak at 262°C, which is just above the crystallization temperature of 250°C. Curve b represents the PEEK sample scanned initially with a very fast rate of  $500^{\circ}\text{C min}^{-1}$  from 250 to 300°C, then followed by a heating rate of  $10^{\circ}\text{C min}^{-1}$  from 300 to 374°C. The purpose of scanning at  $500^{\circ}\text{C min}^{-1}$  between 250 and 300°C was to melt the minor crystal but allow no time for recrystallization to occur during scanning. A direct comparison of curves a and b indicates that the location and area of the main melting peaks are virtually the same. The comparison suggests that when scanned at  $10^{\circ}\text{C min}^{-1}$  the melted minor crystal had no time to recrystallize and remelt at the main melting region, because, if so, the main melting endotherm in curve a would have been different from the main melting endotherm in curve b. Finally, to see how it would change the result, heating of the sample between 250 and 310°C was performed at a slow rate of  $2^{\circ}\text{C min}^{-1}$ . Curve c

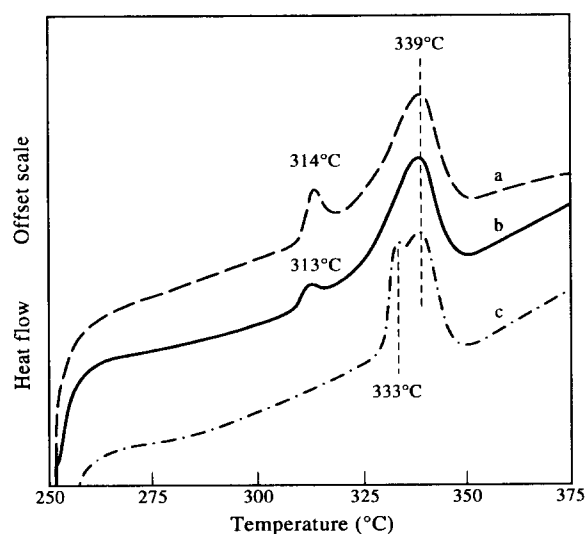


**Figure 5** D.s.c. heating scans ( $10^{\circ}\text{C min}^{-1}$ ) of PEEK samples previously subjected to dynamic heating at various rates or in different temperature ranges: (a) sample A; (b) sample B; (c) sample C

is the d.s.c. scan of a PEEK sample that has been pre-treated by heating at  $2^{\circ}\text{C min}^{-1}$  between 250 and  $310^{\circ}\text{C}$ , then at  $10^{\circ}\text{C min}^{-1}$  from 310 to  $375^{\circ}\text{C}$ . Curve c shows only the last segment of the d.s.c. scan at  $10^{\circ}\text{C min}^{-1}$  from 310 to  $375^{\circ}\text{C}$ . The main melting endotherm is again seen to be the same as that in curve a or curve b. However, a low-temperature peak is observed at about  $315^{\circ}\text{C}$  in addition to the main endotherm. The presence of this minor melting peak at  $313^{\circ}\text{C}$ , which is just above the upper limit of the slow heating temperature range ( $250\text{--}310^{\circ}\text{C}$ ), indicates that the slow heating on the PEEK crystallized at  $250^{\circ}\text{C}$  had the effect of thickening the originally thinner lamellae, but in the mean time leaving the main lamella ( $T_m = 336^{\circ}\text{C}$ ) virtually unchanged. The thickened minor lamellae now melted at a significantly higher temperature of  $313^{\circ}\text{C}$  instead of the original melting at  $262^{\circ}\text{C}$ .

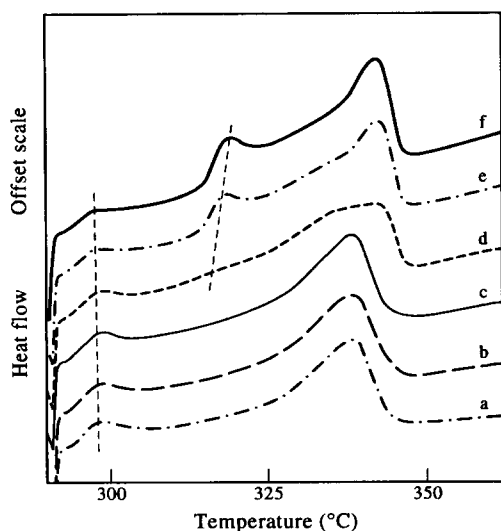
Three additional d.s.c. experiments were performed. A PEEK sample was heated to  $375^{\circ}\text{C}$  to melt the crystal, then quenched to  $250^{\circ}\text{C}$  to become completely amorphous. Subsequently, without allowing any time to crystallize, the sample was immediately scanned at a slow rate of  $2^{\circ}\text{C min}^{-1}$  to  $310^{\circ}\text{C}$ , then quenched back to  $250^{\circ}\text{C}$ . The PEEK sample so treated was labelled sample A. This was then scanned at  $10^{\circ}\text{C min}^{-1}$  from 250 to  $375^{\circ}\text{C}$  to examine its melting behaviour.

Figure 5 shows the d.s.c. scan at  $10^{\circ}\text{C min}^{-1}$  of sample A (curve a). Obviously, sample A prior to the step of heating at  $2^{\circ}\text{C min}^{-1}$  was amorphous, and thus there were no low-temperature minor crystals present at that time. The subsequent heat treatment at  $2^{\circ}\text{C min}^{-1}$  from 250 to  $310^{\circ}\text{C}$  apparently induced non-isothermal crystallization on the originally amorphous liquid. Interestingly, the final scan at  $10^{\circ}\text{C min}^{-1}$  of this sample revealed that the  $2^{\circ}\text{C min}^{-1}$  heat treatment (between 250 and  $310^{\circ}\text{C}$ ) on the originally amorphous PEEK produced a low-temperature crystal that melted at  $314.0^{\circ}\text{C}$ , in addition to the main crystal melting at  $339.5^{\circ}\text{C}$ . A similar result was obtained from sample B, which was subjected to the treatment described for sample A, except that the step of slow heating at  $2^{\circ}\text{C min}^{-1}$  from 250 to  $310^{\circ}\text{C}$  was substituted by a normal heating rate of

$10^{\circ}\text{C min}^{-1}$ . Curve b shows the d.s.c. scan at  $10^{\circ}\text{C min}^{-1}$  for sample B. Again, the d.s.c. scan at  $10^{\circ}\text{C min}^{-1}$  of the sample revealed that the  $10^{\circ}\text{C min}^{-1}$  heat treatment (between 250 and  $310^{\circ}\text{C}$ ) on the originally amorphous PEEK also produced a low-temperature crystal that melted at  $313.0^{\circ}\text{C}$ . The endotherm of this minor peak of sample B, however, is seen to be much smaller than that of sample A. A comparison of the melting enthalpy by area integration showed that the minor endotherm of sample A was larger than that of sample B by about  $5.9\text{ J g}^{-1}$  while the main endotherms for both samples were comparable, suggesting that the slower heating rate ( $2^{\circ}\text{C min}^{-1}$ ) allowed sufficient time for extra chain segments to fold and form more thin lamellae than did the regular heating rate ( $10^{\circ}\text{C min}^{-1}$ ). Sample C was subjected to the same treatments described for sample B, except that the heating at  $10^{\circ}\text{C min}^{-1}$  from 250 to  $310^{\circ}\text{C}$  was substituted by heating at the same rate from 250 to  $330^{\circ}\text{C}$ . Curve c is the d.s.c. scan at  $10^{\circ}\text{C min}^{-1}$  of sample C, showing that the  $10^{\circ}\text{C min}^{-1}$  heat treatment (between 250 and  $330^{\circ}\text{C}$ ) on the originally amorphous PEEK also produced a low-temperature crystal that did not melt at  $313.0^{\circ}\text{C}$ , but instead at  $33.5^{\circ}\text{C}$ . The result suggests that the melting temperature of the minor crystal is continually elevated by the heating scan. Eventually, the originally thin crystals at low temperatures are thickened by the heating process to approach the thickness of the main lamellae and melt finally at  $T_m$  and contribute a small fraction to the main endotherm. The results discussed in Figure 5 have clearly proved the point that melting of a minor thin crystal at a low temperature is not a prerequisite for forming a thick crystal by recrystallization and remelting at a higher temperature.

Bassett *et al.*<sup>24</sup> have shown that minor lamellae are largely confined among dominant lamellar bundles in spherulites. This view is partially supported by an exploratory model<sup>28</sup> recently proposed by us that within a spherulite, the minor crystal entities are thin lamellar branches located between the main skeleton of lamellae. However, our indirect evidence did not rule out the possibility that these later-grown minor lamellae might be more concentrated at the outer periphery of the spherulites. This possibility is supported in a study of Marand and Prasad.<sup>26</sup> Using polarized-light microscopy observation on PEEK, they reached the conclusion that lamellar branches lie in the radial directions and are located on or after the mid-length of the main lamellar bundles. Additionally, some might extend out into the free melt and exist as imperfect interspherulitic crystal-like micelles (aggregates).

It was important to probe whether or not the amount of molecular species available for forming the low-temperature crystal lamellae at an isothermal temperature were influenced by previous crystallization at a higher temperature. Figure 6 shows the six d.s.c. scans at  $10^{\circ}\text{C min}^{-1}$  of the PEEK samples that had been crystallized at  $310^{\circ}\text{C}$  for six different times and then all crystallized at  $290^{\circ}\text{C}$  for 10 min. Curves a–c suggest that crystallization at  $310^{\circ}\text{C}$  for 0, 1 and 2 min, respectively, was not long enough to produce a minor peak above  $310^{\circ}\text{C}$ . However, the minor peak (at about  $295^{\circ}\text{C}$ ) produced by the second-step crystallization at  $290^{\circ}\text{C}$  for 10 min, by contrast, is clearly identified in the d.s.c. thermograms. Curves d–f suggest that crystallization at  $310^{\circ}\text{C}$  for 10, 30 and 60 min, respectively, produced a



**Figure 6** D.s.c. thermograms of PEEK crystallized first at 310°C for various times, then crystallized at 290°C for 10 min. The times at 310°C are: (a) 0 min; (b) 1 min; (c) 2 min; (d) 10 min; (e) 30 min; (f) 60 min

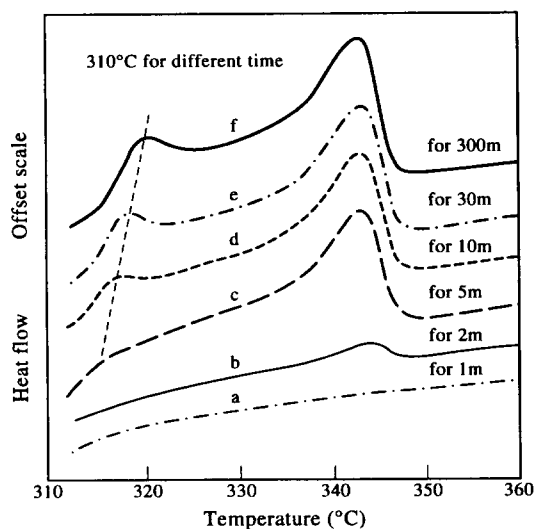


**Figure 7** D.s.c. scans ( $10^{\circ}\text{C min}^{-1}$ ) of PEEK crystallized in a single step at 310°C for various times: (a) 1 min; (b) 2 min; (c) 5 min; (d) 10 min; (e) 30 min; (f) 300 min

minor peak above 310°C. Furthermore, curve f shows that the intensity of the minor peak (at about 295°C) produced by the second-step crystallization at 290°C is least for the PEEK sample that had been crystallized at 310°C for the longest time (60 min). The total amount of polymer molecular species that are available to form low-temperature minor crystals is limited to a constant.

The melting endotherm results of these PEEK samples suggested that the amount of minor crystals were dependent on the time and temperature of crystallization. Figure 7 shows the six d.s.c. scans at  $10^{\circ}\text{C min}^{-1}$  of the PEEK samples that had been crystallized at 310°C for six different times. For the samples crystallized for 1 and 2 min, the d.s.c. scans revealed no minor melting peak and the main melting peak was small and changing with time. The d.s.c. curves of the PEEK samples crystallized for various crystallization times exhibited a main melting endotherm with constant peak

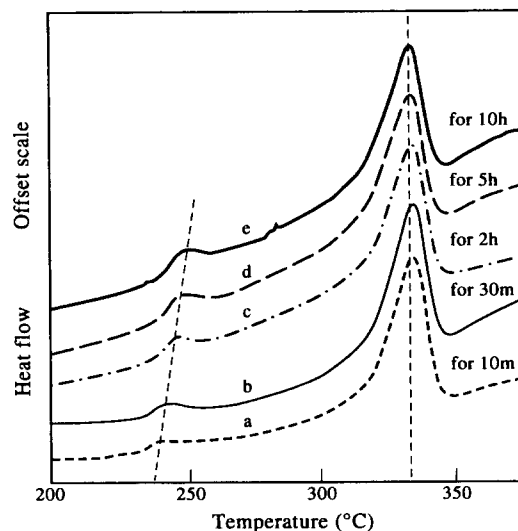


**Figure 8** D.s.c. scans ( $10^{\circ}\text{C min}^{-1}$ ) of PEEK crystallized in a single step at 230°C for various times: (a) 10 min; (b) 30 min; (c) 120 min; (d) 300 min; (e) 600 min

intensity, area and location. However, the minor endothermic peak changed significantly in its intensity and location with increasing time of crystallization.

At other lower crystallization temperatures, similar behaviour was observed in that the melting endotherms of the PEEK samples were dependent on time and temperature of crystallization. Figure 8 shows the five d.s.c. scans at  $10^{\circ}\text{C min}^{-1}$  of the PEEK samples that had been crystallized at 230°C for five different times. Apparently, while the main melting peak remains unchanged, the minor peak increases in intensity and temperature with time. Similar results were obtained at all other isothermal temperatures in the range of 190–310°C.

Figure 9 shows that the peak temperatures of the low-melt lamellae of PEEK increase almost linearly with the logarithm of the annealing/hold time at each of the four relatively low hold temperatures (170, 190, 210 and 230°C). The rate of increase of the low-melt peak temperature seems to be comparable for 170 and 190°C, but becomes slower at the higher isothermal temperatures of 210 and 230°C. If the increase with log(time) is extrapolated to a long enough time, predictably at extended periods of time the minor peak can become high enough to merge with the main melting peak. The main melting peak temperature for the PEEK annealed at these temperature is about 338°C, which is the maximum that the minor peak can reach extended times at low crystallization temperatures. At hold temperatures greater than 230°C, the rate of increase with annealing/hold time becomes smaller with increasing isothermal temperatures<sup>28</sup>. Predictably, if the hold temperature is close to the equilibrium melting temperature of PEEK, the rate of increase in the melting temperature would be near zero. After extended annealing at temperatures close to  $T_m^0$ , the 'minor' and 'major' crystals would no longer be distinguishable, since the originally minor crystal entities have thickened to a thickness comparable to that of the 'major' crystals.

#### Microscopy results

Figure 10 shows the scanning electron micrographs for PEEK samples crystallized at (A) the temperatures and

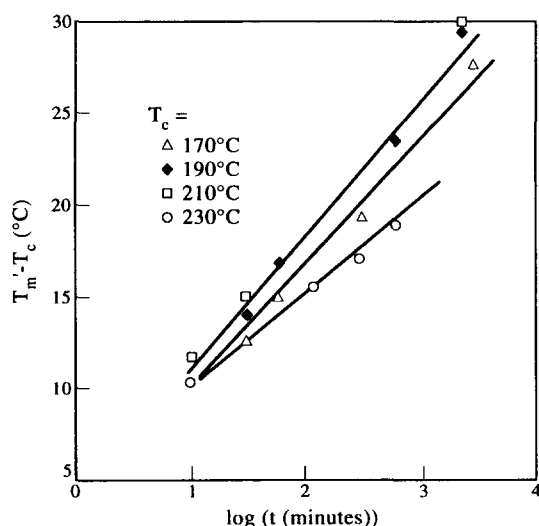


**Figure 9** The increase of the minor melting peak temperature,  $\Delta(T'_m - T_c)$ , as a function of logarithm of annealing time at four isothermal temperatures

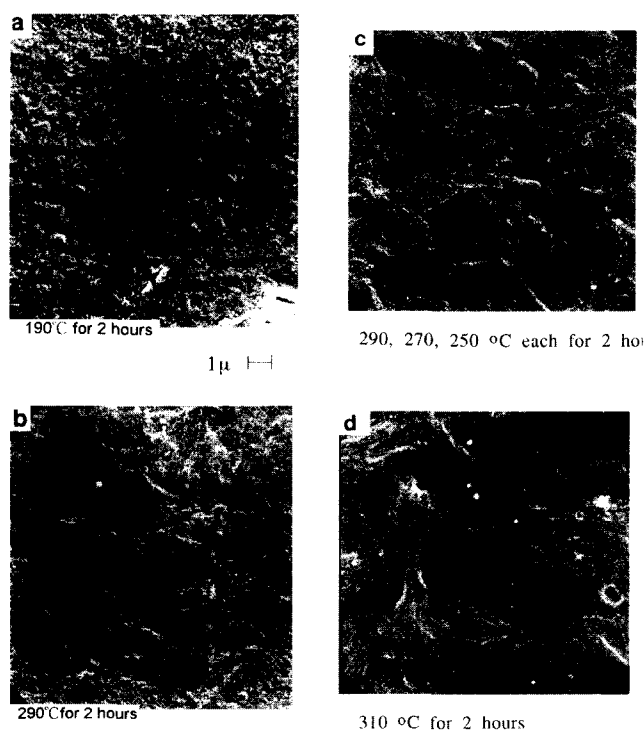
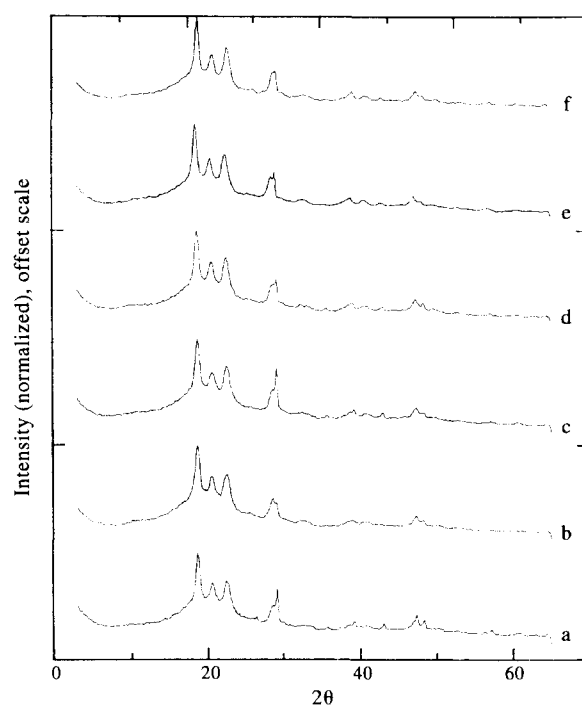


**Figure 10** Micrographs for PEEK samples crystallized at (a) 190°C for 2 h; (b) 290°C for 2 h; (c) 290, 270 and 250°C for 2 h each; (d) 310°C for 2 h

times indicated. Micrograph A shows that crystallization at 190°C for 2 h yielded only relatively small spherulites of about 2–3  $\mu\text{m}$ . The melting of this sample showed a minor peak (at 207°C) and a main melting peak (at 339°C). Micrograph B shows that crystallization at 290°C for 2 h yielded considerably larger spherulites (about 5–7  $\mu\text{m}$ ) with visibly thicker lamellar bundles. Micrograph C shows that the spherulite dimensions remained about the same for the PEEK sample annealed at 270 and 250°C (2 h each) in addition to the prior crystallization at 290°C for 2 h. The fact that the main lamellar bundles are about the same in micrographs B and C suggests that the main lamellae did not thicken as



Wide angle X-ray diffraction for PEEK

**Figure 11** X-ray crystallographs of the PEEK samples crystallized for 30 min in a single step at various isothermal temperatures: (a) 310°C; (b) 290°C; (c) 270°C; (d) 250°C; (e) 230°C; (f) 210°C

a result of additional annealing at 270 and 250°C. However, the lamellar branches are denser for micrograph C, indicating that additional annealing at 270 and 250°C did produce additional minor crystal lamellae between the main lamellar bundles. By comparison, micrograph D shows that crystallization at 310°C for 2 h yielded only much larger spherulites of about 10  $\mu\text{m}$ . The melting of this sample, from d.s.c. measurements, revealed a minor peak (320°C) and a main melting peak (342°C). Micrograph D shows that, for the PEEK crystallized at 310°C the lamellar bundles are not dense but appear to be uniformly thick, indicating that the minor crystal lamellae ( $T'_m = 320^\circ\text{C}$ ) have thickened to dimensions comparable with the main lamellae ( $T_m = 342^\circ\text{C}$ ) and therefore they are not easily distinguishable any more. Although the resolution in the scanning electron micrographs is not comparable to that in transmission electron microscopy (TEM), the SEM results in this study showed a clear trend of variation of the lamellar bundles in the PEEK samples after different thermal treatments.

#### X-ray results

Figure 11 compares the X-ray crystallography results of PEEK samples crystallized in a single step at various isothermal temperatures. Dawson and Blundell<sup>29</sup> have reported the diffraction peaks for PEEK at  $2\theta = 18.7^\circ$ ,  $20.7^\circ$ ,  $22.6^\circ$  and  $28.7^\circ$ , for (1 1 0), (1 1 3), (2 0 0) and (2 1 3) planes, respectively. The figure shows that there is no discernible difference in these crystallographs, indicating that the unit cells remained unchanged regardless of the presence of the minor crystal lamellae in addition to the main lamellae due to crystallization at these temperatures. X-ray experiments were also performed on multiple-temperature crystallized PEEK samples. The results

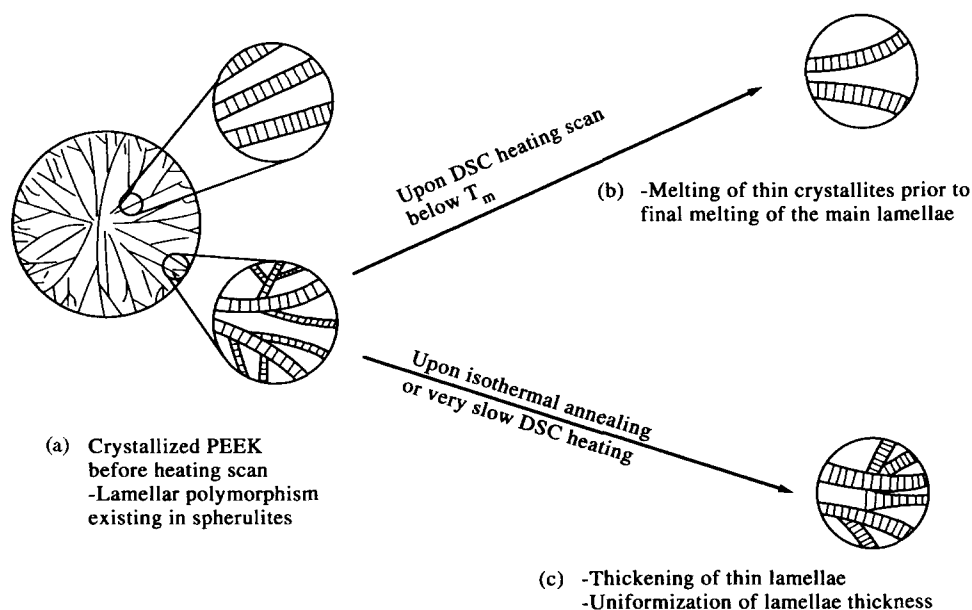


**Figure 12** Simplified schematic diagram showing thick and thin lamellae existing in the spherulites of crystallized PEEK and subsequent changes upon heating or stepwise annealing

showed that the peak positions were all the same, indicating that the unit cell of the lower-melting crystal aggregates remained the same. The crystallographs are not shown here for brevity.

Gardner *et al.*<sup>30</sup> have demonstrated two different unit cell packings in poly(ether ketone) (PEK) and poly(ether ketone ketone) (PEKK) when cold- or melt-crystallized. By comparison, our X-ray results have shown that the unit cell in PEEK is apparently not altered by the imposed thermal histories. Morphological changes are likely in the lamellar scales. Recently, several laboratories have also attempted to obtain *in situ* information of morphological changes during crystallization and melting at the lamellar level using time-resolved small-angle X-ray scattering or WAXD measurements<sup>31–33</sup>. Hopefully, these newly developed techniques, if coupled with the special sample preparation and thermal analysis used in this study, will provide better information in resolving the issue.

Figure 12 shows a schematic representation of the lamellar morphology of crystallized PEEK and possible changes upon dynamic heating at various rates or upon isothermal annealing. The d.s.c. SEM and X-ray results discussed so far have undoubtedly suggested that PEEK crystallization followed by annealing at multiple isothermal temperatures can cause an extra small fraction of polymer chain segments to fold into low-temperature thin crystallites that are not stable with time or temperature and can thicken as the time of isothermal hold increases or as a result of dynamic heating scans. At high heating scan rates, the low-temperature crystallites already formed simply melt and exhibit the observed low-temperature endotherm peaks between  $T_c$  and the main  $T_m$ . However, at low enough scanning rates, the originally thin crystallites can thicken gradually to form thicker lamellae as the polymer is heated up during scanning. The scan-thickened lamellae then eventually melt and contribute to a small extent to the main endotherm of the main crystallites originally present.

#### Modelling for sequential growth

We have previously proposed a schematic model for the description of primary and secondary (minor) crystal growth in the different crystallization stages for poly(*p*-phenylene sulfide) (PPS)<sup>34</sup>. It was expected that the model could be similarly used to describe the spherulitic morphology of PEEK with lamellae of multiple thickness distributions. Within an idealized spherulite, the minor crystal entities are actually thin lamellar branches located in the outer periphery of spherulites or exist as imperfect interspherulite crystal-like micelles highly impinged by the growing front of spherulites. The well-known Avrami equation<sup>35</sup> was found to deviate significantly from the experimental data at the later stage of crystallization for PEEK. To more accurately describe the crystallization kinetics of PEEK, it was proposed that the growth of the primary crystal (crystal I) originally proceeded from the very beginning ( $t = 0$ ), then was followed by a sequential growth of the secondary crystal (crystal II) at  $t = \tau$ , which took place in parallel with the still-growing primary crystal (crystal I). The Avrami equation was used to describe the crystallization in each segment of the crystallization, by incorporating a modification to allow for the description of series-parallel growth of the major and minor crystal lamellae. The result is expressed as the following two equations, each describing one of the two stages of crystallization<sup>34</sup>.

Stage I crystallization, before  $t = \tau$ :

$$X_{t1} = 1 - \exp(-k_1 t^{n_1}) \quad (1)$$

$$X_t = X_{t1}$$

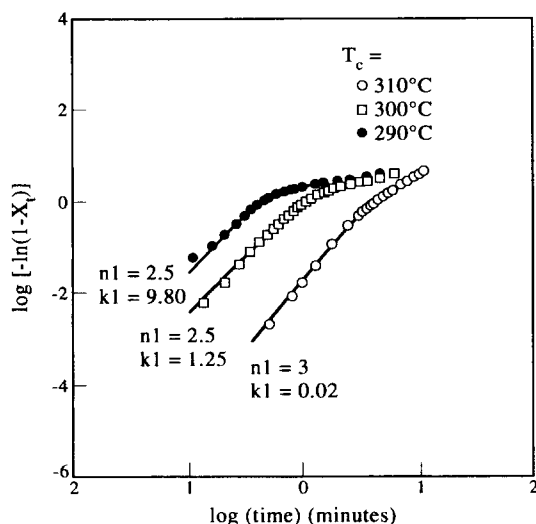
which produces only the major crystal.

Stage 2 crystallization, after  $t = \tau$ :

$$X_{t2} = \omega_1 [1 - \exp(-k_1 t^{n_1})] + \omega_2 [1 - \exp(-k_2 (t - \tau)^{n_2})] \quad (2)$$

**Table 1** Kinetic parameters for PEEK sequential crystallization model

$T_c$ ( $^{\circ}\text{C}$ )	$\omega_1$	$k_1$	$n_1$	$\omega_2$	$k_2$	$n_2$	$\tau$ (min)
310	0.80	0.02	3.0	0.20	0.04	1.0	4.0
300	0.84	1.25	2.5	0.16	0.60	1.0	1.5
290	0.85	9.80	2.5	0.15	1.10	1.0	1.0

**Figure 13** Sequential series-parallel crystallization model showing fit with the experimental data for PEEK

which produces minor crystal aggregates (II) in parallel with the still-growing (but largely diminished) major crystal (I) extending from stage 1. The overall crystallinity is described by  $X_t = X_{t1} + X_{t2}$ . In these two equations, the constants bear the same meanings as those in the Avrami equation, except that the subscript '1' refers to the first stage and '2' refers to the later (second) stage of crystallization. According to equation (1), only primary crystallization takes place in the first stage. Subsequently in the later (second) stage, according to equation (2), additional crystallization of the minor crystal (designated 'II') starts at a later time ( $\tau$ ) which proceeds in parallel with the still-continuing crystallization of the primary crystal (designated 'I'). In equation (2),  $\omega_1$  and  $\omega_{11}$  are the weight factors for the primary and minor crystals, respectively, as the crystallization enters the second stage. The weight fractions for crystal I and crystal II grown after  $\tau$  were readily calculated from the ratio of melting enthalpy of the primary and secondary crystals produced at the time of the second stage of crystallization.

Figure 13 shows that the series-parallel crystallization model (equations (1) and (2)) gives a good description of the crystallization of PEEK from the beginning until near completion. Since the first stage of crystallization was entirely populated by the primary crystal, the kinetic constants, including the exponent  $n_1$ , could be readily obtained experimentally from the Avrami plots using the early-stage crystallization data. When the crystallization entered the second stage at  $t = \tau$ , the kinetic constants for the crystallization of the primary crystal should remain the same; however, the secondary crystal appeared in this stage and joined in parallel with the primary crystal. The only assumption made here was

that the crystallization of the secondary crystal after  $t = \tau$  could be described with a highly nucleated heterogeneous process with a line growth mechanism (exponent = 1.0). All the kinetic constants (Table 1) derived for this model are seen to be reasonable, suggesting a realistic physical meaning of this modelling. In this descriptive model,  $t = \tau$  was taken directly from the d.s.c. result of the first appearance of the minor crystal, which agreed with the time of the location of the discontinuity ( $t_d$ ) in the Avrami plots. The only kinetic constant that needed to be estimated for the model was  $k_{2,11}$  for the crystallization of the secondary crystal in the later stage.

The successful description of this model helped confirm our earlier suggestion that the crystallized PEEK indeed possesses lamellae of multiple thickness distribution. Crystallization at an isothermal temperature produces not only a regular main crystal, but also a thin crystal that can melt at temperatures slightly above the crystallization temperature and that can also thicken and melt at the main  $T_m$ . Furthermore, crystallization followed by annealing at lower temperatures can yield more thin lamellae. The two types of crystals grow independently. Consequently the thin lamellae lag behind the main lamella in their appearance, thus they develop in parallel with the growth of the main lamella in the later stage. Kinetically, the main lamella is the fastest growing, while the thin lamellae, being subjected to restraints, progress at slower rates than the main lamella during crystallization.

## CONCLUSION

We propose that the multiple melting in PEEK is associated with lamellae of multiple thicknesses or multiple populations of minor crystal aggregates. Lamellar thickening is a phenomenon occurring inevitably as a result of dynamic heating at slow enough rates or annealing at a temperature for a long enough time. The multiple melting phenomenon of PEEK observed during d.s.c. heating scans is attributed to the melting of thin lamellae of variable thickness co-existing with the main lamella of a larger thickness. Upon crystallization at an isothermal temperature, the thick main crystallite with the highest melting point is always the first formed, with the thin low-temperature lamellae starting to develop at a time when the growth of the main crystallite is near to completion.

Furthermore, our results have demonstrated that both thin crystalline lamellae of multiple thickness distributions and a main crystallite develop sequentially in the first stage and in parallel growth in the later stage of crystallization or annealing treatments. To prove this, a sequential parallel-series crystallization model has been found to describe the crystallization kinetics well. The successful modelling of the kinetics by using the sequential parallel-series crystallization mechanism suggests that these low-melting crystal entities are probably confined between major lamellae and their growth occurs after the major lamellae are almost fully developed in the spherulites.

## ACKNOWLEDGEMENT

Financial support (NSC 83-0405-E006-029) is provided



by the National Science Council (NSC) of the Republic of China.

## REFERENCES

- 1 Lee, Y. and Porter, R. S. *Polym. Eng. Sci.* 1985, **26**, 633
- 2 Jones, D. P., Leach, D. C. and Moore, D. P. *Polymer* 1985, **26**, 1385
- 3 Nguyen, H. X. and Ishida, H. *Polym. Compos.* 1987, **57**, 1987
- 4 Desio, G. P. and Rebenfeld, L. *J. Appl. Polym. Sci.* 1992, **44**, 1989
- 5 Seferis, J. C. *Polym. Compos.* 1986, **7**, 158
- 6 Chung, J. S. and Cebe, P. *J. Polym. Sci., Part B, Polym. Phys.* 1992, **30**, 163
- 7 Crevecoeur, G. and Groeninckx, G. *Macromolecules* 1991, **24**, 1190
- 8 Holdsworth, P. and Turner-Jones, A. *Polymer* 1971, **12**, 195
- 9 Alfonso, G. C., Pedemonte, E. and Ponzetti, L. *Polymer* 1979, **20**, 104
- 10 Boon, J., Challa, G. and van Krevelen, D. W. *J. Polym. Sci., Polym. Phys. Edn* 1968, **6**, 1791
- 11 Woo, E. M. and Ko, T. Y. *Colloid Polym. Sci.* in press
- 12 Wunderlich, B. in 'Macromolecular Physics', Academic Press, New York, Vol. 2, 1976
- 13 Roberts, R. C. *Polymer* 1969, **10**, 113
- 14 Blundell, D. J. *Polymer* 1987, **28**, 2248
- 15 Lee, Y., Porter, R. S. and Lin, J. S. *Macromolecules* 1989, **22**, 1756
- 16 Lee, Y. and Porter, R. S. *Macromolecules* 1987, **20**, 1336
- 17 Chang, S. S. *Polym. Commun.* 1988, **29**, 138
- 18 Nichols, M. E. and Robertson, R. E. *J. Polym. Sci., Part B, Polym. Phys.* 1992, **30**, 755
- 19 Kim, J., Nichols, M. E. and Robertson, R. E. *J. Polym. Sci., Part B, Polym. Phys.* 1994, **32**, 887
- 20 Mai, K., Zhang, M., Zeng, H. and Qi, S. *J. Appl. Polym. Sci.* 1994, **51**, 57
- 21 Huo, P. and Cebe, P. *Colloid. Polym. Sci.* 1992, **270**, 840
- 22 Cebe, P. and Chung, S. *Polym. Compos.* 1990, **11**, 265
- 23 Blundell, D. J. and Osborn, B. N. *Polymer* 1983, **24**, 953
- 24 Bassett, D. C., Olley, R. H. and Al-Raheil, I. A. M. *Polymer* 1988, **29**, 1745
- 25 Cheng, S. Z. D., Wu, Z. Q. and Wunderlich, B. *Macromolecules* 1987, **20**, 2802
- 26 Marand, H. and Prasad, A. *Macromolecules* 1992, **25**, 1731
- 27 Lovinger, A. J., Hudson, S. D. and Davies, D. D. *Macromolecules* 1992, **25**, 1752
- 28 Chen, C.-Y. and Woo, E. M. *Polym. J.* 1995, **27**, 361
- 29 Dawson, P. C. and Blundell, D. J. *Polymer* 1980, **21**, 577
- 30 Gardner, K. H., Hsiao, B. S. and Faron, K. L. *Polymer* 1994, **35**, 2290
- 31 Wang, J., Alvarez, M., Zhang, W., Wu, Z., Li, Y. and Chu, B. *Macromolecules* 1992, **25**, 6934
- 32 Kruger, K. N. and Zachmann, H. G. *Macromolecules* 1992, **26**, 5202
- 33 Hsiao, B. S., Gardner, K. H., Wu, D. Q. and Chu, B. *Polymer* 1993, **34**, 3986, 3996
- 34 Woo, E. M. and Chen, J. M. *J. Appl. Polym. Sci.* 1995, **33**, 1985
- 35 Avrami, M. *J. Chem. Phys.* 1949, **9**, 177